JACS
JOURNAL OF THE AMERICAN CHEMICAL SOCIETY

Communication

pubs.acs.org/JACS

Synthetic Control of FePtM Nanorods (M = Cu, Ni) To Enhance the Oxygen Reduction Reaction

Huiyuan Zhu,[†,§] Sen Zhang,[†,§] Shaojun Guo,[†] Dong Su,[‡] and Shouheng Sun*[,†]

[†]Department of Chemistry, Brown University, Providence, Rhode Island 02912, United States

[‡]Center for Functional Nanomaterials, Brookhaven National Laboratory, Upton, New York 11973, United States

Supporting Information

ABSTRACT: To further enhance the catalytic activity and durability of nanocatalysts for the oxygen reduction reaction (ORR), we synthesized a new class of 20 nm × 2 nm ternary alloy FePtM (M = Cu, Ni) nanorods (NRs) with controlled compositions. Supported on carbon support and treated with acetic acid as well as electrochemical etching, these FePtM NRs were converted into core/shell FePtM/Pt NRs. These core/shell NRs, especially FePtCu/Pt NRs, exhibited much improved ORR activity and durability. The $Fe_{10}Pt_{75}Cu_{15}$ NRs showed a mass current densities of 1.034 A/mg_{Pt} at 512 mV vs Ag/AgCl and 0.222 A/mg_{Pt} at 557 mV vs Ag/AgCl, which are much higher than those for a commercial Pt catalyst (0.138 and 0.035 A/mg_{Pt}, respectively). Our controlled synthesis provides a general approach to core/shell NRs with enhanced catalysis for the ORR or other chemical reactions.

Developing highly efficient catalysts for the oxygen reduction reaction (ORR) is a key to the fabrication of commercially viable fuel cell devices and metal−air batteries for future energy applications.[1−3] The recent search for advanced catalysts for the ORR has led to some exciting advances in our understanding of the catalytic nature, allowing more rational tuning of the catalytic properties via controlled syntheses. For example, when Pt is alloyed with an early transition metal such as Fe, Co, or Ni, its d-band center is downshifted and its bonding to oxygenated species is weakened, leading to an increase in catalytic activity for the ORR.[3−5] More interestingly, when Pt is present as a thin shell in a core/shell structure, both its activity and durability are greatly enhanced as a result of the simultaneous downshift of its d-band center and surface strain induced in the Pt shell, which is favorable for O_2 adsorption and activation.[6−8] Pt catalysis for the ORR can be further activated when Pt catalysts are prepared in a controlled shape,[9,10] especially in a one-dimensional (1D) nanostructure,[8,9] where interactions between a crystal facet and oxygenated species as well as the carbon support can be optimized to achieve high catalytic activity with increased catalyst stability. These previous studies indicated that a 1D core/shell nanostructure with Pt in the shell can combine both alloy and shape effects to enhance ORR catalysis. Therefore, a controlled synthesis of 1D core/shell nanostructures may provide a new approach to highly efficient Pt catalysts for the ORR.

Here we report the synthesis of core/shell nanorods (NRs) to provide a further enhancement of ORR catalysis. We recently prepared FePt, CoPt, and FePtPd nanowires (NWs) and studied their catalysis of the ORR.[11,12] We found that adding Pd to FePt NWs destabilized the catalyst without an obvious activity gain. Conversely, these ternary NWs increased the activity for the methanol oxidation reaction.[11] Without the presence of Pd, the FePt and CoPt NWs were more active and durable for the ORR than polyhedral nanoparticle (NP) catalysts.[12] However, upon acetic acid (AA) treatment to remove the surfactant coating and activate the NW catalyst, a majority of M in the MPt NWs was etched away, minimizing the effect of M on the enhancement of Pt catalysis. To realize fully the M-alloy benefits in catalysis, it was necessary to develop a 1D nanostructure in which M is preserved in acid solution. With this in mind, we developed a controlled synthesis of 20 nm × 2 nm NRs of FePtM (M = Cu, Ni) and studied their acid stability. We found that these thin FePtM NRs, especially FePtCu NRs, are much more stable in acid solution. When treated with AA and etched electrochemically in 0.1 M $HClO_4$, these ternary alloy NRs were converted into core/shell FePtM/Pt NRs with Fe and M (especially Cu) being preserved in the NR cores, as illustrated in Figure 1. These core/shell NRs combine 1D shape and core/shell effects on catalysis and indeed show much higher activity and durability for the ORR.

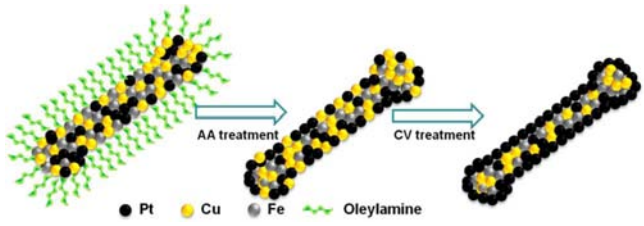

Figure 1. Schematic illustration of the formation and activation of the core/shell-type FePtCu/Pt NR catalyst.

FePtM (M = Cu, Ni) NRs were synthesized by the thermal decomposition of iron pentacarbonyl [$Fe(CO)_5$] and the reduction of metal acetylacetonates [$Pt(acac)_2$ and $M(acac)_2$] [see the Supporting Information (SI)].[12] Oleylamine and sodium oleate were used to control the NR growth and

Received: March 26, 2013
Published: May 1, 2013

dx.doi.org/10.1021/ja403041g | J. Am. Chem. Soc. 2013, 135, 7130−7133

stabilization, while a 2/3 (v/v) mixture of oleylamine and octadecene served as the solvent. In the synthesis, the composition of the ternary NRs was controlled by the precursor ratios. Inductively coupled plasma atomic emission spectroscopy (ICP-AES) analyses indicated that the M/Pt ratio in the as-synthesized NRs was directly proportional to the $M(acac)_2/Pt(acac)_2$ ratio (Table S1 in the SI). $Fe_{51}Pt_{49}$ NRs were also made without the addition of $M(acac)_2$ (Figure S1 in the SI) and were used as a control. Transmission electron microscopy (TEM) images showed that the as-synthesized FePtM (M = Cu, Ni) NRs with different compositions had the same morphology, with an average length of 20 ± 2 nm and an average diameter of 2 ± 0.2 nm (Figures 2A and S2). These

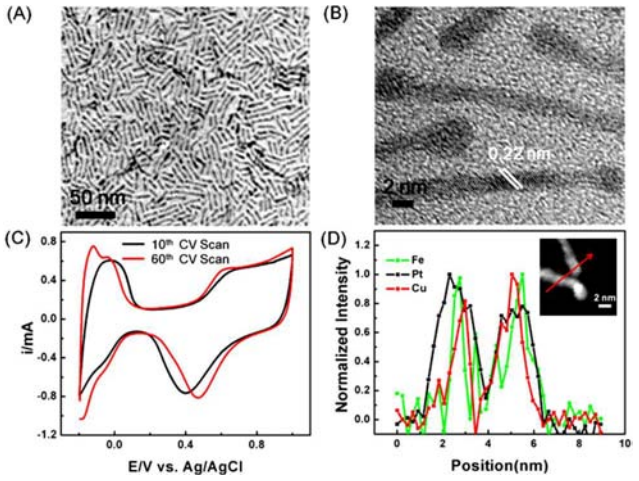

Figure 2. (A) TEM image of the 20 × 2 nm $Fe_{29}Pt_{41}Cu_{30}$ NRs. (B) HRTEM image of $Fe_{29}Pt_{41}Cu_{30}$ NRs. (C) CV scans at the beginning and end of the electrochemical etching process of the NRs from (A) after AA washing. The potential ranged from −0.2 to 1.0 V vs Ag/AgCl at a scan rate of 100 mV/s in N_2-saturated 0.1 M $HClO_4$. (D) HAADF−STEM image (inset) and STEM−EELS line scan of the representative $Fe_{10}Pt_{75}Cu_{15}$ NRs obtained after after AA washing and CV cycling of $Fe_{29}Pt_{41}Cu_{30}$ NRs.

FePt and FePtM NRs showed typical face-centered cubic (fcc) structures, as indicated by the X-ray diffraction patterns in Figure S3. Figure 2B shows a high-resolution TEM (HRTEM) image of the representative $Fe_{29}Pt_{41}Cu_{30}$ NRs, within which the lattice spacing was measured to be 0.22 nm, corresponding to the (111) interplanar distance of fcc FePtCu. The lattice fringes point away from the NR growth direction by approximately 55°, indicating that the NRs grow along the [100] direction, consistent with the behavior observed in the growth of FePt and FePtPd NWs.[11−13]

Under the current synthetic conditions, 1D FePt NRs were first formed before the Cu or Ni precursor was added at 160 °C (Figure S4). It appears that the FePt NRs served as the template and Cu/Ni was incorporated into the NR structure via intermetallic diffusion.[14] The presence of $Fe(CO)_5$ and the formation of FePt was the key to the formation of ternary NRs. Without $Fe(CO)_5$, only irregular MPt (M = Cu, Ni) NPs were produced. When the FePtM NRs were prepared using equimolar amounts of Fe and Pt precursor (0.25 mmol each), the addition of Cu/Ni precursor had no effect on the FePt formation, as the Fe/Pt ratios in the FePt and FePtM NRs were nearly the same. When the Fe/Pt precursor ratio was increased to 2:1 (0.5 mmol/0.25 mmol), the Fe/Pt ratio remained at 1:1 (Figure S5). In this case, the Cu/Ni salt was mainly reduced by $Fe(CO)_5$ when excess $Fe(CO)_5$ was present. However, with both $Fe(CO)_5$ and $Pt(acac)_2$ at 0.25 mmol, Cu/Ni salt tended to be reduced by oleylamine. The subsequent high-temperature (240 °C) aging promoted the atomic diffusion, producing ternary alloy NRs. We should note that although the excess $Fe(CO)_5$ had no obvious effect on the final NR composition, it did help to control the length of the NRs. For example, an Fe/Pt precursor ratio of 2:1 led to the formation of 60 nm × 2 nm NWs (Figure S5).

The 20 × 2 nm NRs were loaded on a Ketjen carbon support (C) as reported previously.[15,16] The supported NRs (C-NRs) were washed with AA at 70 °C to remove the oleate/oleylamine coating.[17] ICP-AES analyses showed that this acid treatment led to partial loss of Fe in all of the NRs and Ni in the FePtNi NRs but negligible loss of Cu in the FePtCu NRs (Table S2). After the washing step, the C-NRs (or commercial C−Pt NPs, 20% mass loading with Pt NP diameters of 2.5−3.5 nm) were suspended in 4/1 (v/v) deionized water/isopropanol containing 5% Nafion, forming a suspension containing 2 mg of catalyst/mL. A 20 μL aliquot of the suspension was deposited on the glassy carbon (GC) surface of a rotating disk electrode (RDE) and dried in the ambient environment. The C-NRs deposited on the GC-RDE were subjected to further cyclic voltammetry (CV) scanning from −0.2 to 1.0 V vs Ag/AgCl in N_2-saturated 0.1 M $HClO_4$ for "Cu dealloying".[18] Figure 2C shows the CV scans after the 10th and 60th potential cycles for the $Fe_{12}Pt_{54}Cu_{34}$ NRs obtained by AA washing of the $Fe_{29}Pt_{41}Cu_{30}$ NRs shown in Figure 2A,B. The CV scan for the 60th cycle shows a sharper hydrogen underpotential formation/stripping peak in the range from −0.2 to 0.15 V vs Ag/AgCl and a positive shift of the reduction peak related to oxygenated Pt species, suggesting Cu depletion in the near-surface region and the formation of a Pt-enriched shell.[19−21] After these CV scans, the NR composition was changed from $Fe_{12}Pt_{54}Cu_{34}$ to $Fe_{10}Pt_{75}Cu_{15}$. The core/shell FePtCu/Pt NRs were characterized by atomically resolved aberration-corrected high-angle annular dark-field scanning transmission electron microscopy (HAADF−STEM) and STEM−electron energy loss spectroscopy (STEM−EELS). Figure 2D shows the HAADF−STEM image of the NRs after 60 CV cycles (inset) and the related STEM−EELS line scan, confirming the formation of a thin Pt shell after surface dealloying.

Figure 3A shows CV scans of the core/shell C−FePtCu/Pt NRs obtained from $Fe_{29}Pt_{41}Cu_{30}$ NRs and of the C−Pt NPs in N_2-saturated 0.1 M $HClO_4$. The peaks in the range from −0.2 to 0.15 V vs Ag/AgCl are from the common hydrogen underpotential formation/stripping and can be used to estimate the electrochemically active surface area (ECASA) of the catalyst.[22] The metal oxidation/reduction peaks appear in the range from 0.4 to 0.9 V vs Ag/AgCl. The composition-dependent ORR activity of the FePtCu NRs was studied. Figure 3B shows the ORR polarization curves of the core/shell FePtCu/Pt NRs and the commercial Pt NPs in O_2-saturated 0.1 M $HClO_4$. The ORR polarization curves depict the diffusion-limiting current region ranging from −0.05 to 0.4 V vs Ag/AgCl and the mixed kinetic−diffusion-controlled region between ∼0.4 and ∼0.7 V vs Ag/AgCl. With increasing amount of Cu, the half-wave potential of the FePtCu NRs shifted positively, indicating that the NRs with the initial composition of $Fe_{29}Pt_{41}Cu_{30}$ (0.557 V vs Ag/AgCl) have better ORR catalytic activity than the $Fe_{38}Pt_{42}Cu_{20}$ (0.551 V vs Ag/AgCl), $Fe_{42}Pt_{44}Cu_{14}$ (0.537 V vs Ag/AgCl), and $Fe_{51}Pt_{49}$ NRs (0.520 V vs Ag/AgCl) at the same NR loading by weight. The ORR

dx.doi.org/10.1021/ja403041g | J. Am. Chem. Soc. 2013, 135, 7130−7133

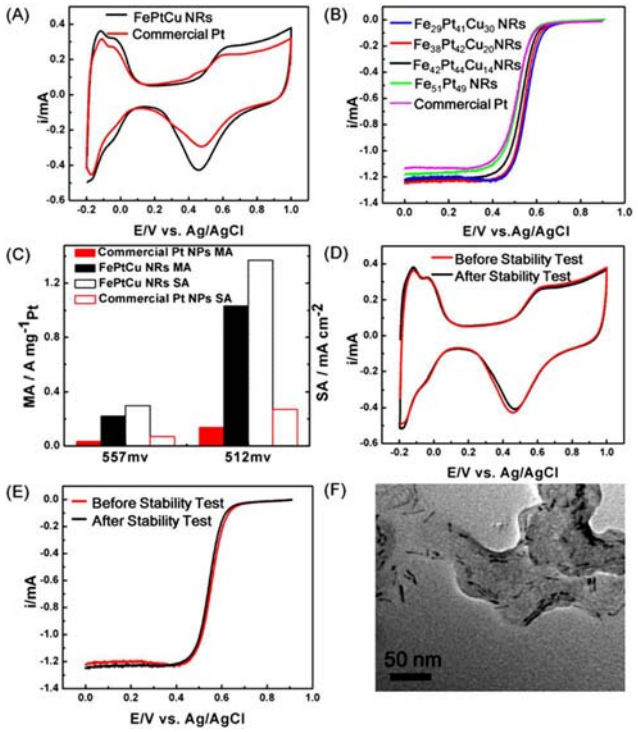

Figure 3. (A) CVs of the C−$Fe_{10}Pt_{75}Cu_{15}$ NRs and C−Pt NPs in N_2-saturated 0.1 M $HClO_4$ at a scan rate of 50 mV/s. (B) Polarization curves for FePtCu NRs with different initial compositions and commercial Pt NPs in O_2-saturated 0.1 M $HClO_4$ at 295 K. (C) ORR mass activities (MA) and specific activities (SA) of $Fe_{10}Pt_{75}Cu_{15}$ NRs and commercial Pt NPs. (D) CVs of $Fe_{10}Pt_{75}Cu_{15}$ NRs in N_2-saturated 0.1 M $HClO_4$ before and after 5000 potential cycles between 0.4 and 0.8 V in O_2-saturated 0.1 M $HClO_4$. (E) Polarization curves of the $Fe_{10}Pt_{75}Cu_{15}$ NRs in O_2-saturated 0.1 M $HClO_4$ at 295 K before and after 5000 potential cycles between 0.4 and 0.8 V vs Ag/AgCl in O_2-saturated 0.1 M $HClO_4$. (F) TEM image of the $Fe_{10}Pt_{75}Cu_{15}$ NRs on the carbon support after the 5000-cycle stability test.

activity of the $Fe_{10}Pt_{75}Cu_{15}$ NRs was compared with that of the C−Pt NPs (Figure 3C). The ORR half-wave potential of the $Fe_{10}Pt_{75}Cu_{15}$ NRs is 45 mV more positive than that of the C−Pt catalyst (0.512 V vs Ag/AgCl). The $Fe_{10}Pt_{75}Cu_{15}$ NRs have a mass activity (MA) of 1.034 A/mg_{Pt} and a specific activity (SA) of 1.369 mA/cm^2 at 512 mV vs Ag/AgCl, which are 7 and 5 times higher than those of the commercial C−Pt NPs (0.138 A/mg_{Pt} and 0.271 mA/cm^2, respectively). At 557 mV vs Ag/AgCl, the $Fe_{10}Pt_{75}Cu_{15}$ NRs have an MA of 0.222 A/mg_{Pt} and an SA of 0.299 mA/cm^2, while those of the commercial C−Pt are only 0.035 A/mg_{Pt} and 0.068 mA/cm^2, respectively.

The durability of the core/shell NR catalyst was tested by cycling the potential between 0.4 and 0.8 V vs Ag/AgCl at a sweep rate of 100 mV/s in O_2-saturated 0.1 M $HClO_4$. The CVs (Figure 3D) and polarization curves (Figure 3E) of the $Fe_{10}Pt_{75}Cu_{15}$ NRs before and after 5000 potential cycles nearly overlap. Correspondingly, the core/shell NRs showed no obvious morphology or composition changes after the durability test, as demonstrated by TEM (Figure 3F) and their slight composition drop in Fe and Cu from $Fe_{10}Pt_{75}Cu_{15}$ to $Fe_8Pt_{78}Cu_{14}$. These results suggest that the FePtCu/Pt core/shell NRs are highly stable under the current ORR conditions.

The FePtNi NRs also displayed composition-dependent ORR activities (Figure S6), as the presence of more FeNi in the FePtNi NRs led to higher activity. However, after the AA treatment, a substantial amount of Ni was lost (Table S2). Therefore, FePtNi NRs were less stable in acid and less active for catalyzing the ORR than FePtCu NRs.

In summary, we have developed a facile solution-phase process to synthesize ternary alloy FePtM (M = Cu, Ni) NRs with dimensions controlled to be 20 nm × 2 nm and compositions tuned by the precursor ratios. These NRs are more stable in acid than their binary counterparts. When treated with acetic acid and electrochemical etching in 0.1 M $HClO_4$, these ternary alloy NRs were converted into core/shell-structured FePtM/Pt NRs. These core/shell NRs, especially the FePtCu/Pt NRs, are a new class of ORR catalysts that are superior to their binary counterparts and the commercial Pt NP catalyst. The core/shell NRs obtained from the $Fe_{29}Pt_{41}Cu_{30}$ alloy NRs show much enhanced durability and have mass and specific activities that are 7- and 5-fold higher than those of the commercial Pt NP catalyst. Our controlled synthesis of core/shell 1D nanostructures provides a new approach to highly efficient Pt catalysts for the ORR. The same structure may also offer an alternative catalyst model to study electronic and strain effects for tuning NP catalysis for other chemical reactions.

■ ASSOCIATED CONTENT

Supporting Information

FePtM (M = Cu, Ni) and FePt NR synthesis, characterization, and electrochemical measurements. This material is available free of charge via the Internet at http://pubs.acs.org.

■ AUTHOR INFORMATION

Corresponding Author

ssun@brown.edu

Author Contributions

[§]H.Z. and S.Z. contributed equally.

Notes

The authors declare no competing financial interest.

■ ACKNOWLEDGMENTS

This work was supported by the U.S. Army Research Laboratory and the U.S. Army Research Office under the Multi University Research Initiative (MURI) (Grant W911NF-11-1-0353 on "Stress-Controlled Catalysis via Engineered Nanostructures"). Electron microscopy work carried out at the Center for Functional Nanomaterials at Brookhaven National Laboratory was supported by the U.S. Department of Energy, Office of Basic Energy Sciences, under Contract DE-AC02-98CH10886.

■ REFERENCES

(1) Zhang, J. *PEM Fuel Cell Electrocatalysts and Catalyst Layers: Fundamentals and Applications*; Springer: London, 2008.

(2) Wang, C.; Daimon, H.; Onodera, T.; Koda, T.; Sun, S. *Angew. Chem., Int. Ed.* **2008**, *47*, 3588−3591.

(3) Lee, H.; Habas, S. E.; Kweskin, S.; Butcher, D.; Somorjai, G. A.; Yang, P. *Angew. Chem., Int. Ed.* **2006**, *45*, 7824−7828.

(4) (a) Sethuraman, V. A.; Weidner, J. W.; Haug, A. T.; Motupally, S.; Protsailo, L. V. *J. Electrochem. Soc.* **2008**, *155*, B50−B57. (b) Adz, R. R.; Wang, J. X. *J. Phys. Chem. B* **1998**, *102*, 8988−8993. (c) Wanjala, B. N.; Fang, B.; Luo, J.; Chen, Y.; Yin, J.; Engelhard, M. H.; Loukrakpam, R.; Zhong, C. J. *J. Am. Chem. Soc.* **2011**, *133*, 12714−12727.

(5) Stamenkovic, V. R.; Mun, B. S.; Arenz, M.; Mayrhofer, K. J. J.; Lucas, C. A.; Wang, G.; Ross, P. N.; Markovic, N. M. *Nat. Mater.* **2007**, *6*, 241−247.

(6) Mazumder, V.; Chi, M.; More, K. L.; Sun, S. *J. Am. Chem. Soc.* **2010**, *132*, 7848−7849.
(7) Wang, C.; Vliet, D.; More, K.; Zaluzec, N.; Peng, S.; Sun, S.; Daimon, H.; Wang, G.; Greeley, J.; Pearson, J.; Paulikas, A.; Karapetrov, G.; Strmcnik, D.; Markovic, N. M.; Stamenkovic, V. R. *Nano Lett.* **2011**, *11*, 919−926.
(8) (a) Cui, C.-H.; Yu, S.-H. *Acc. Chem. Res.* **2013**, DOI: 10.1021/ar300254b. (b) Cui, C.; Li, H.; Yu, J.; Gao, M.; Yu, S. *Angew. Chem., Int. Ed.* **2010**, *49*, 9149−9152. (c) Li, H.; Cui, C.; Zhao, S.; Yao, H.; Gao, M.; Fan, F.; Yu, S. *Adv. Energy Mater.* **2012**, *2*, 1182−1187. (d) Koenigsmann, C.; Santulli, A. C.; Gong, K.; Vukmirovic, M. B.; Zhou, W.; Sutter, E.; Wong, S. S. *J. Am. Chem. Soc.* **2011**, *133*, 9783−9795.
(9) Zhou, H.; Zhou, W.; Adzic, R. R.; Wong, S. S. *J. Phys. Chem. C* **2009**, *113*, 5460−5466.
(10) Sun, S.; Zhang, G.; Geng, D.; Chen, Y.; Li, R.; Cai, M.; Sun, X. *Angew. Chem., Int. Ed.* **2011**, *50*, 422−426.
(11) Guo, S.; Zhang, S.; Sun, X.; Sun, S. *J. Am. Chem. Soc.* **2011**, *133*, 15354−15357.
(12) Guo, S.; Li, D.; Zhu, H.; Zhang, S.; Markovic, N. M.; Stamenkovic, V. R. *Angew. Chem., Int. Ed.* **2013**, *52*, 3465−3468.
(13) Wang, C.; Hou, Y.; Kim, J.; Sun, S. *Angew. Chem., Int. Ed.* **2007**, *46*, 6333−6335.
(14) Liu, S.; Zhang, C.; Yuan, L.; Bao, J.; Tu, W.; Han, M.; Dai, Z. *Part. Part. Syst. Charact.* **2013**, DOI: 10.1002/ppsc.201200150.
(15) Mazumder, V.; Sun, S. *J. Am. Chem. Soc.* **2009**, *131*, 4588−4589.
(16) Zhang, S.; Guo, S.; Zhu, H.; Su, D.; Sun, S. *J. Am. Chem. Soc.* **2012**, *134*, 5060−5063.
(17) Guo, S.; Sun, S. *J. Am. Chem. Soc.* **2012**, *134*, 2492−2495.
(18) Koh, S.; Anniyev, T.; Greeley, J.; More, K.; Yu, C.; Liu, Z.; Strasser, P. *Nat. Chem.* **2010**, *2*, 458−460.
(19) Wang, C.; Chi, M.; Li, D.; Strmcnik, D.; Wang, G.; Komanicky, V.; Markovic, N. M; Stamenkovic, V. R. *J. Am. Chem. Soc.* **2011**, *133*, 14396−14403.
(20) Stamenkovic, V. R.; Fowler, B.; Mun, B. S; Wang, G.; Ross, P. N; Lucas, C. A.; Markovic, N. M. *Science* **2007**, *315*, 493−497.
(21) Maillard, F.; Dubau, L.; Durst, J.; Chatenet, M.; Andre, J.; Rossinot, E. *Electrochem. Commun.* **2010**, *12*, 1161−1164.
(22) Snyder, J.; Fujita, T.; Chen, M. W.; Erlebacher, J. *Nat. Mater.* **2010**, *9*, 904−907.